The Structure in Mesonic Channels above T_c
Lattice results
from the QCD-TARO Collaboration

Quark-antiquark 4-point correlation functions in the mesonic channels at non-zero temperature are studied by a complex of methods to obtain insight into the hadronic and plasma physics of QCD.

We consider propagation in Euclidean *time* (temperature) direction, trying to extract *pole masses* and further structure of the *spectral functions*.
By also allowing the quarks to get apart in the *space* direction we measure mesonic *wave functions*, providing hereto unique results.

The methods employed include

- building various correlators (ultra-local or smeared, in particular using mesonic wave functions) and analyze their *time* evolution,
- fits of the spectral functions with pole and Breit-Wigner *ansätze* adequate for $T > 0$ (KMS condition),
- direct extraction of the spectral function using singular value decomposition and maximal entropy method (MEM),
- calculation of static quark potential, etc.

We attempt a careful discussion of the physical problems involved and of the limitations of the various methods. Because of the uncertainties of the problem, this is a necessary step in asserting the significance of the results.

THE BASIS OF THE DISCUSSION: Non-zero temperature QFT in imaginary time formalism
(adequate for the lattice studies):

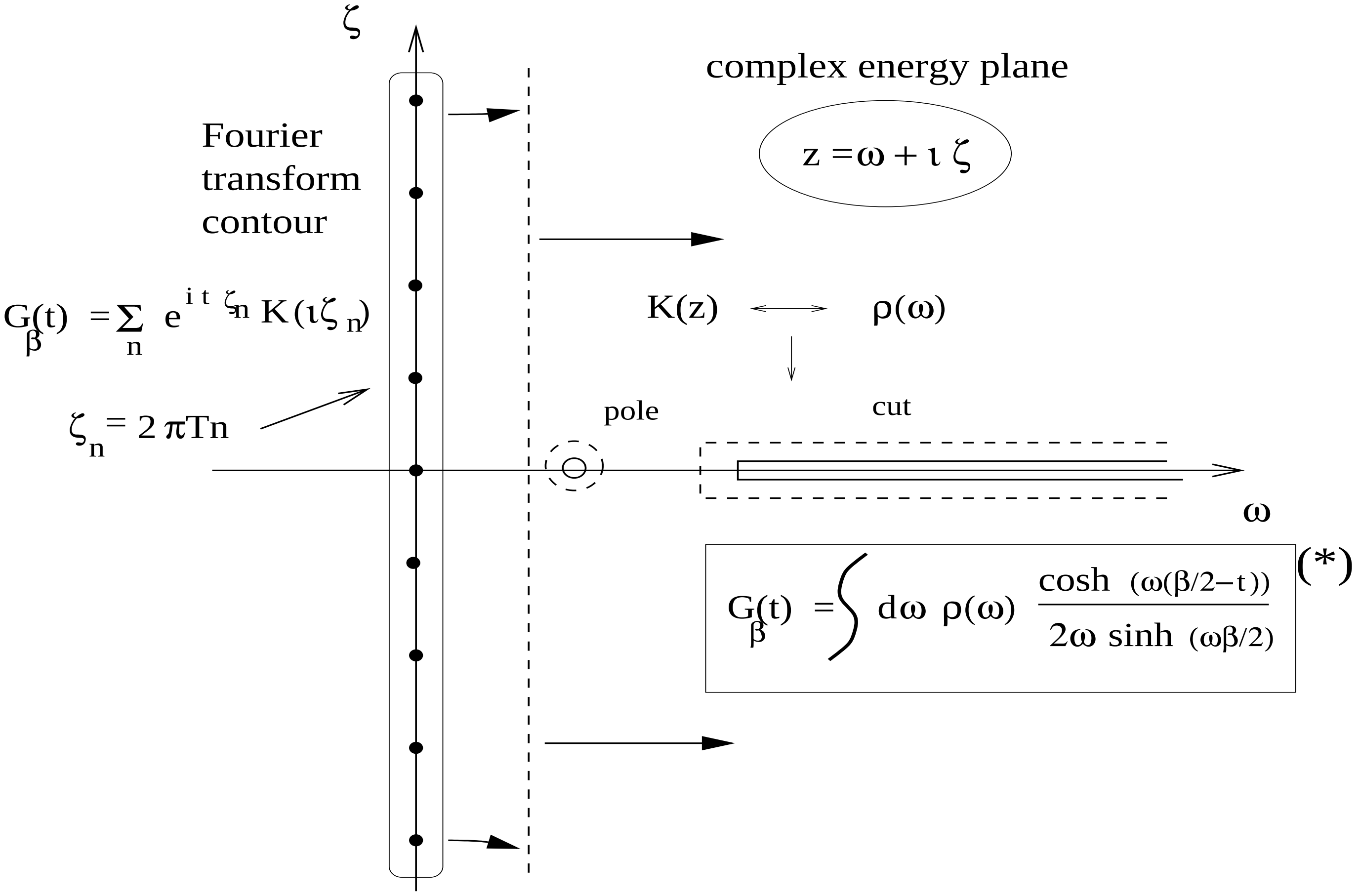

Figure 1: Complex energy plane with analytic continuation.

A thermal propagator $G_\beta(t)$ is related by analytic continuation to the spectral function $\rho(\omega)$ and hence to the Minkowski propagator. We can write down an integral equation for $\rho(\omega)$ and fit its structure with the data for $G_\beta(t)$.

Depending on the operator used to construct the meson (smearing, etc) and on the temperature the quantum states content of the propagator varies. This shows up in the spectral function ρ.

The integral equation for ρ represents a typical "ill-posed problem" and needs therefore "regularization" by physical (e.g., fit ansatz) or other kind of "a priori information" (e.g., statistical bias: Bayesian procedures).

Notice that on the *finite lattice* the momentum is discretized, therefore also the "continuum" part of $\rho(\omega)$ is given by a series of discrete contributions.

THE QUANTITIES MEASURED are general 4-point functions (temporal propagators are important since they involve the original dynamics).

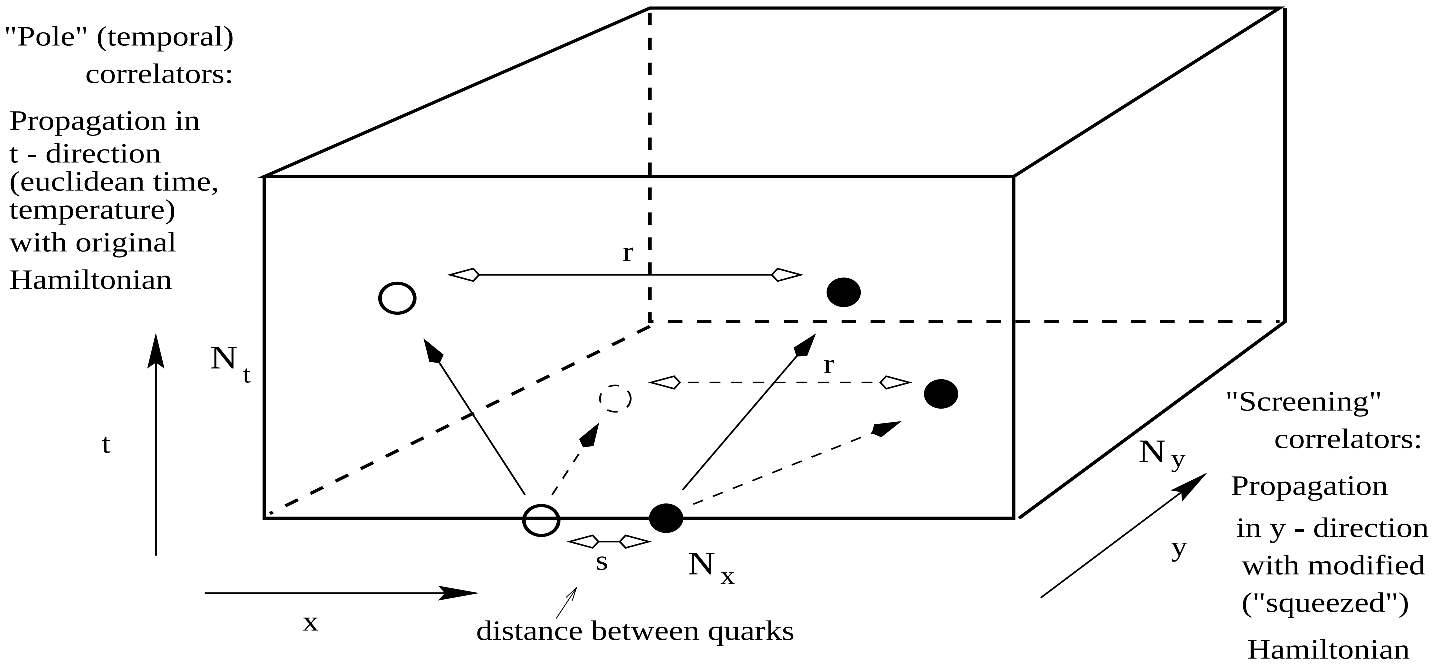

Figure 2: Mesonic correlators

$$\langle [\bar{q}(\vec{r}_1,t)\,\Gamma_{\rm h}\,q(\vec{r}_2,t)]^{\dagger}\ \bar{q}(\vec{s}_1,0)\Gamma_{\rm h}q(\vec{s}_2,0)\rangle = \langle \gamma_5\,S(\vec{s}_1,0;\vec{r}_1,t)\,\gamma_5\,\Gamma_{\rm h}\,S(\vec{s}_2,0;\vec{r}_2,t)\,\Gamma_{\rm h}\rangle$$

S : quark propag., $\Gamma_{\rm h}$: γ_5 (ps.scalar), γ_i (vector), 1 (sc.), $\gamma_5\,\gamma_i$ (ax. vect.)

The dependence on $R = r_1 + r_2$ can be used to project fixed total momentum, the dependence on $r_1 - r_2 = r$ is used for the "wave function" $\phi(r;t)$ at t.

s_1, s_2 can be used to construct adequate initial states (sources) Φ^{Γ}_{w}:

$$\Phi^{\Gamma}_{w}(0) = \sum_{\vec{s}_1,\vec{s}_2} w(\vec{s}_1,\vec{s}_2)\,\bar{q}(\vec{s}_1,0)\Gamma_{\rm h}q(\vec{s}_2,0), \quad G^{\Gamma}_{w}(r,t) = \sum_{\vec{R}} \langle [\bar{q}(\vec{r}_1,t)\,\Gamma_{\rm h}\,q(\vec{r}_2,t)]^{\dagger}\ \Phi^{\Gamma}_{w}(0)\rangle$$

$$= \sum_{\vec{R}} \sum_{\vec{s}_1,\vec{s}_2} w(\vec{s}_1,\vec{s}_2)\,\langle \gamma_5\,S(\vec{s}_1,0;\vec{r}_1,t)\,\gamma_5\,\Gamma_{\rm h}\,S(\vec{s}_2,0;\vec{r}_2,t)\,\Gamma_{\rm h}\rangle \qquad (**)$$

$$\begin{aligned} \text{Smearing function} : w(\vec{x}_1,\vec{x}_2) &= \delta(\vec{x}_1)\,\delta(\vec{x}_2) && \text{point} - \text{point (ultra} - \text{local)} \\ &= \delta(\vec{x}_1)\,{\rm e}^{-a\,|x_2|^p} && \text{point} - \exp \\ &= {\rm e}^{-a\,|x_1|^p}\,{\rm e}^{-a\,|x_2|^p} && \exp - \exp \\ &= 1 && \text{wall} \end{aligned}$$

GENERAL PROBLEMS

physical aspects:

- QGP $\longrightarrow$ new effective degrees of freedom,
- change in the symmetry properties (chiral symmetry restoration),
- deconfining/screening transition, change in the dynamics.

aspects of the analysis:

- t is limited ($t \leq \beta = 1/T < \infty$) $\longrightarrow$ low energy information is rough and obscured by high energy excitations;
- the state admixture is physically relevant (temperature effect) and the correlator (and hence $\rho(\omega)$) depends on the mesonic operator Φ_w;
- the inversion of (*) is not unique (ill-posedness, limited information for the RHS on finite lattice, statistical errors) $\longrightarrow$ results for ρ may strongly depend on regularization;
- the analysis is done for **quenched QCD** $\longrightarrow$ incomplete dynamics (lacks pair creation), *it seems to catch the essential part, however.*

Procedure:

- identify mesons Φ_w by using the ground state wave function in the source and study their properties as function of temperature T;
- study source dependence (hence the excited state admixture) *vs* T;
- solve the integral eq. (*) for ρ for various sources
  - by using singular value decomposition and MEM;
  - by using physical *ansätze* for ρ;
- compare with unbound quark hypothesis (perturbative plasma);
- check the static quark potential, glue properties, etc.

SIMULATIONS

We use anisotropic lattices in order to have a finer discretization of the t-axis and increase the information. The anisotropy calibration is done at $T = 0$ using static potential and mesonic propagators.

We use various sources to probe the mesonic channels. The $exp - exp$ *(ee)* - source is tuned slightly wider than the wave function of the meson at $T = 0$. We also use wider *(wall)* and narrower *(ep)* and *(pp)* sources.

We use Coulomb gauge. We compare with free quark propagation in the same channels: $G_0(t)$ obtained using free quark propagators S_0 in (**).

Dimensionfull quantities are understood as given in units of a_σ or a_τ.

We quote results from:

Simulation I: Anisotropic lattice $12^3 \times N_\tau$, $a_\tau = a_\sigma/5.3 \simeq (4.5GeV)^{-1}$
Wilson Y-M, Wilson fermions, "light" quarks $(m_{ps} \sim 0.5GeV)$
$N_\tau \; = \; 72, \; 20, \; 16, \; 12 \quad \longrightarrow \; T \; \simeq \;$ "0", 0.93, 1.13, 1.5 $\times T_c$

[QCD-TARO: Ph. de Forcrand, M. García Pérez, T. Hashimoto, S. Hioki, H. Matsufuru, O. Miyamura, A. Nakamura, I.-O. Stamatescu, T. Takaishi and T. Umeda : PR D 63 (2001) 054501]

Simulation II: Anisotropic lattice $16^2 \times 24 \times N_\tau$, $a_\tau = a_\sigma/3.95 \simeq (6.4GeV)^{-1}$
Symanzik improved Y-M, Wilson fermions, "charm" quarks $(m_{ps} \sim 3GeV)$
$N_\tau \; = \; 96, \; 26, \; 22, \; 16 \quad \longrightarrow \; T \; \simeq \;$ "0", 0.93, 1.1, 1.52 $\times T_c$

[Umeda,Katayama,Matsufuru,Miyamura: N.Ph.(P.S.) 94 (2001) 435, hep-lat/0011085]

Simulation III: Anisotropic lattice $20^3 \times N_\tau$, $a_\tau = a_\sigma/4 \simeq (8GeV)^{-1}$
Symanzik improved Y-M, $\mathcal{O}(a)$ improved Wilson fermions, "charm" quarks $(m_{ps} \sim 2.8GeV)$
$N_\tau \; = \; 160, \; 64, \; 32, \; 27, \; 26, \; 24, \; 20, \; 14 \; \longrightarrow$
$T \; \simeq \;$ "0", 0.45, 0.89, 1.06, 1.10, 1.19, 1.43, 2.04 $\times T_c$

[Umeda,Nomura,Matsufuru: hep-lat/0209139 and in preparation]

MESON PROPAGATORS AND POLE MASSES

To extract the physical signal we use the "effective mass" $M(t)$ from:

$$G(t) \simeq \cosh\left(\left(\frac{N_\tau}{2} - t\right) M(t)\right)$$

See (**). $M(t)$ is essentially the local slope of the propagator and shows more sensitively the structure in the propagators (while the later may look similar to each other). A flat $M(t) = M$ indicates that the propagator is dominated by a low energy pole at mass $\simeq M$.

At $T = 0$ the *(ee)* source is very flat. All sources agree at large t.

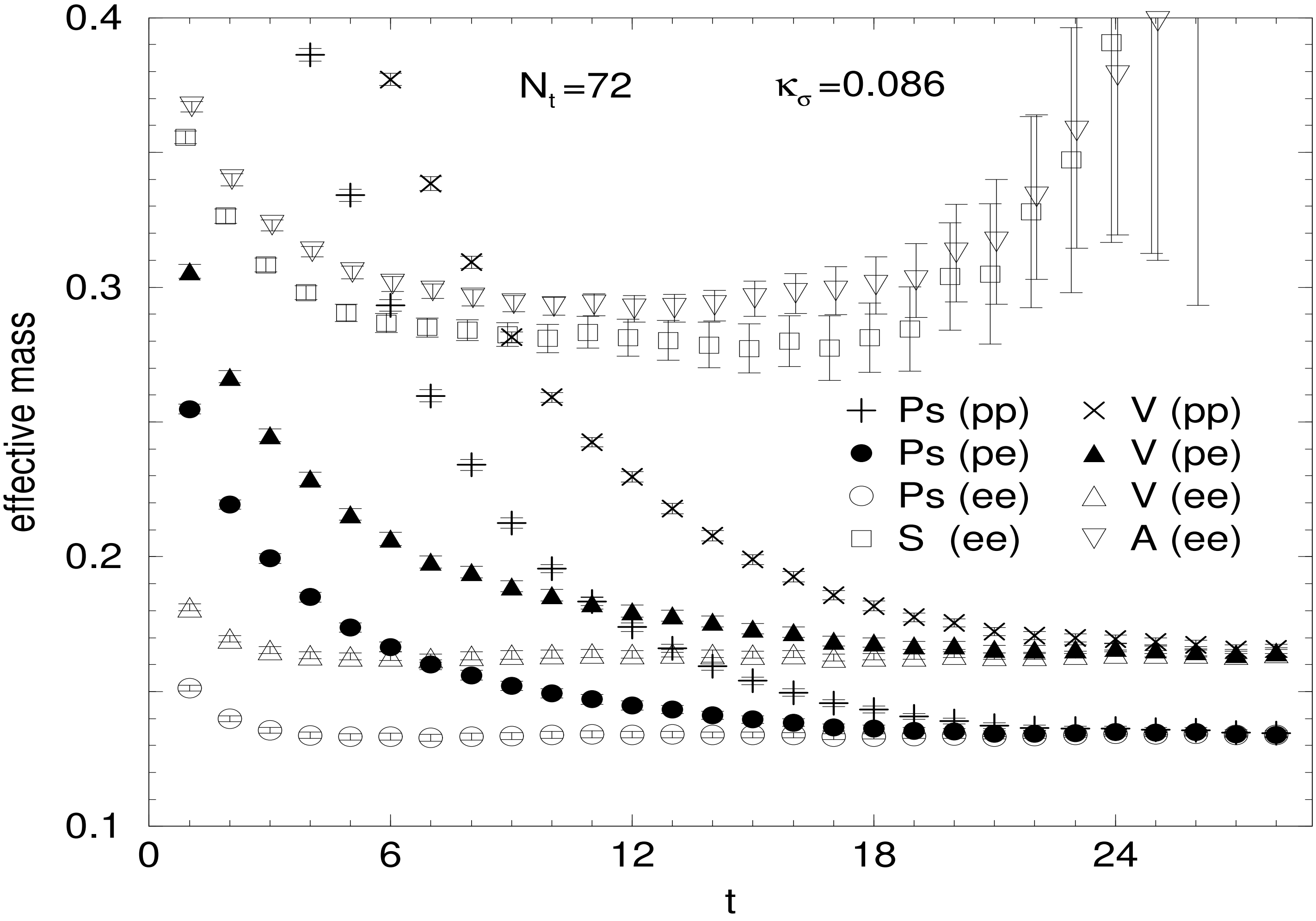

Figure 3: $T = 0$ effective masses $M(t)$ from *Simulation I* for various mesonic channels and sources. The wall source is not ploted here (for it $M(t)$ is not flat but rising from below). The asymptotic value of $M(t)$ is $\simeq$ pole mass.

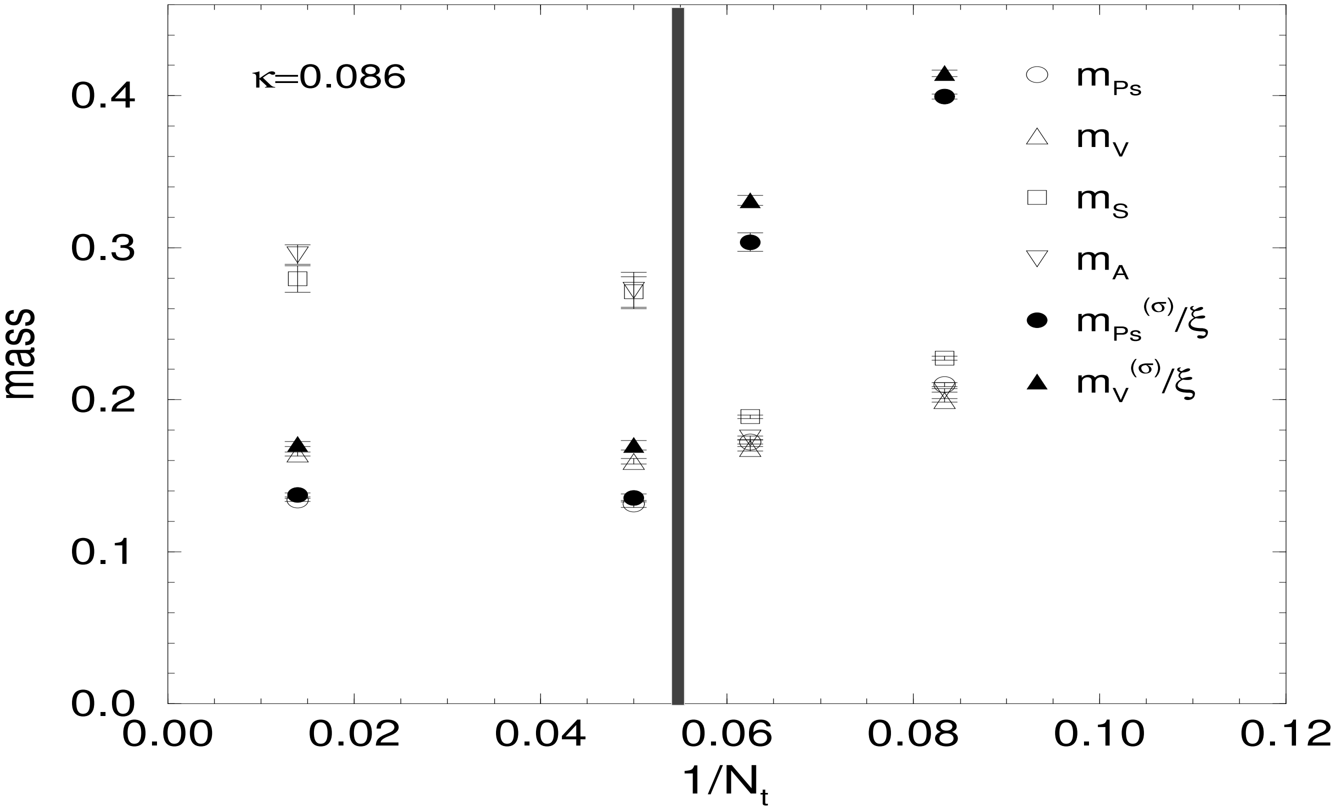

Figure 4: Lowest masses propagating in the ps, V, S and A channels *vs* T (full symbols are "screening" masses). The vertical line indicates T_c.

Summary of results for meson propagators (masses)

$\underline{T < T_c}$: small or no difference to $T = 0$ for both light and charm mesons.

$\underline{T > T_c}$: effective masses depend increasingly (with T) on t and source $\longrightarrow$ *no longer only one narrow state* (wide structure, excited states). Thereby:

- we see *similar* *and* *dissimilar* features with free quark propagation;
- considering the smallest "masses" in various channels we observe:
  - for charm mesons: *practically constant* masses (with T);
  - for light mesons: *chiral symmetry restoration at* T_c and *linear increase with* T *above* T_c.

MESON WAVE FUNCTION

We calculate Coulomb gauge wave functions from correlators (**) with various initial states (sources) and $q\ \bar{q}$ in final state at spatial distance r:

$$\varphi(r,t) = \frac{G(r,t)}{G(0,t)}$$

Again we compare with the $\varphi_0(r,t)$ from free quark propagators S_0 in $G(r,t)$.

First trial: we use the (ee) source (which was tuned slightly wider than the *measured* w.f. at $T = 0$). For bound quarks the shape of the w.f. should stabilize with increasing t, for unbound quarks it should become flatter.

Second trial: we use various sources and measure the *average* r as function of t, and the t - dependence of $\varphi(r,t)$ at fixed r.

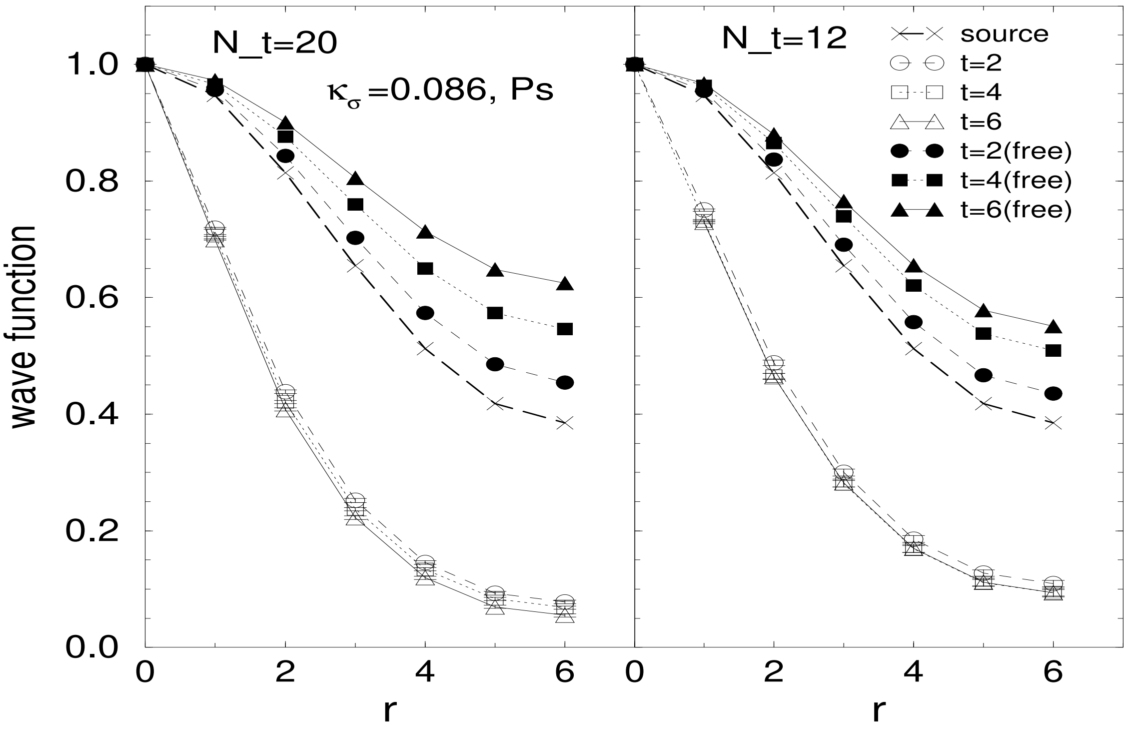

Figure 5: Pseudoscalar wave function $\varphi(r,t)$ for light quarks (*Simulation I, (ee)* source) at $T \simeq 0.93$ and $1.5\,T_c$ (from left to right) at $t = 2$, 4 and 6. The free "wave function" $\varphi_0(r,t)$ (full symbols) flattens, as it should, while the meson wave function stabilizes rapidly. Expected below T_c (where we know that there is a bound state), *above T_c this is a non-trivial result.*

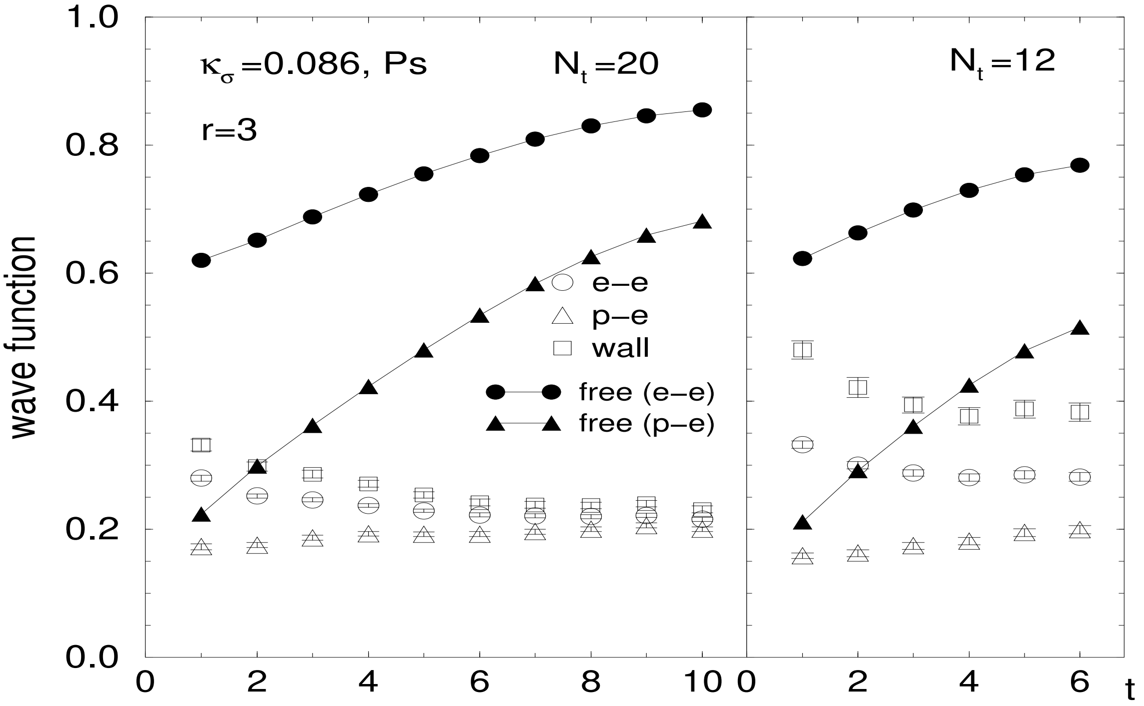

Figure 6: Evolution of the pseudoscalar wave function $\varphi(r,t)$ with t at fixed $r=3$: light quarks (*Simulation I*) at $T \simeq 0.93$ and $1.5\,T_c$ (from left to right), for wide (*wall*), mesonic (*ee*) and narrow (*pe*) sources. The free "wave function" $\varphi_0(r,t)$ (full symbols) flattens in all case (for *wall* it is just 1 independently on t), while for meson narrow initial states widen, wide ones narrow, tending to stabilize with increasing t (at a common value below T_c, not yet reached above T_c).

Summary of wave function results. Both for "light" and charm quarks: **below and above** T_c we observe:

- stabilization with increasing t: well defined wave function $\simeq \exp(-ax^p)$ with mesonic parameters a, p,
- the *source dependence* increases with T,
- striking difference to unbound quarks at all T.

Thus even at $1.5\,T_c$ *quarks are spatially correlated* (for times of at least $1/T$) $\longrightarrow$ suggests *metastable* $q\,\bar{q}$ states in the low energy region of the mesonic channels above T_c.

MESONIC SPECTRAL FUNCTION: Results from *Simulation III*

Correlators (**) are measured for two types of *ps* and vector meson operators: point (*pp*) source and sink, and smeared (*ee*) source and sink.

The solution of (*) is attempted by 2 methods:

<u>I. MEM</u>: inversion of the integral equation using singular value decomposition and maximal entropy method to obtain the $\rho(\omega)$ which maximize a Lyapunov function constrained both by the data and by statistical criteria (maximal entropy of the ansatz):

$$\begin{aligned} Q[\rho;\alpha] &= \alpha S[\rho] - L[\rho] \\ S[\rho] &= \int_0^\infty d\omega \left[\rho(\omega) - \rho_{DM}(\omega) - \rho(\omega)\,\log\left(\frac{\rho(\omega)}{\rho_{DM}(\omega)}\right)\right], \end{aligned}$$

where L is the likelihood function involving the data. Thereby:

- the parameter α is eliminated by averaging over the results at given α with a certain probability distribution;
- the expected asymptotic behaviour of $\rho(\omega)$ is taken into account by the "default model"

  $$\rho_{DM}(\omega) = m_{DM}\,\omega^2$$

  leaving a free parameter m_{DM}, to be used for stability checks.

<u>II. Fit</u> of the data with various ansätze for the spectral function: narrow states (poles) and wide states (modified Breit-Wigner)

$$\rho_{BW} = \frac{\omega^2\, m\,\gamma}{(\omega^2 - m^2)^2 + m^2\gamma^2}$$

In both cases tests are performed by varying the fit interval, number of data points etc. and also by checking against the known results for free quarks.

Tests for "free quark" mesons

Quarks with the same action and mass as used in the simulation (improved Wilson, $m_q \simeq 0.98 GeV$) but here in trivial gauge field are used to construct the *ps* meson propagator. The corresponding spectral function ρ_0 is discrete because of quantized *spatial* momenta. The propagator is then used to recalculate the spectral function both by the I. MEM and II. Fit methods.

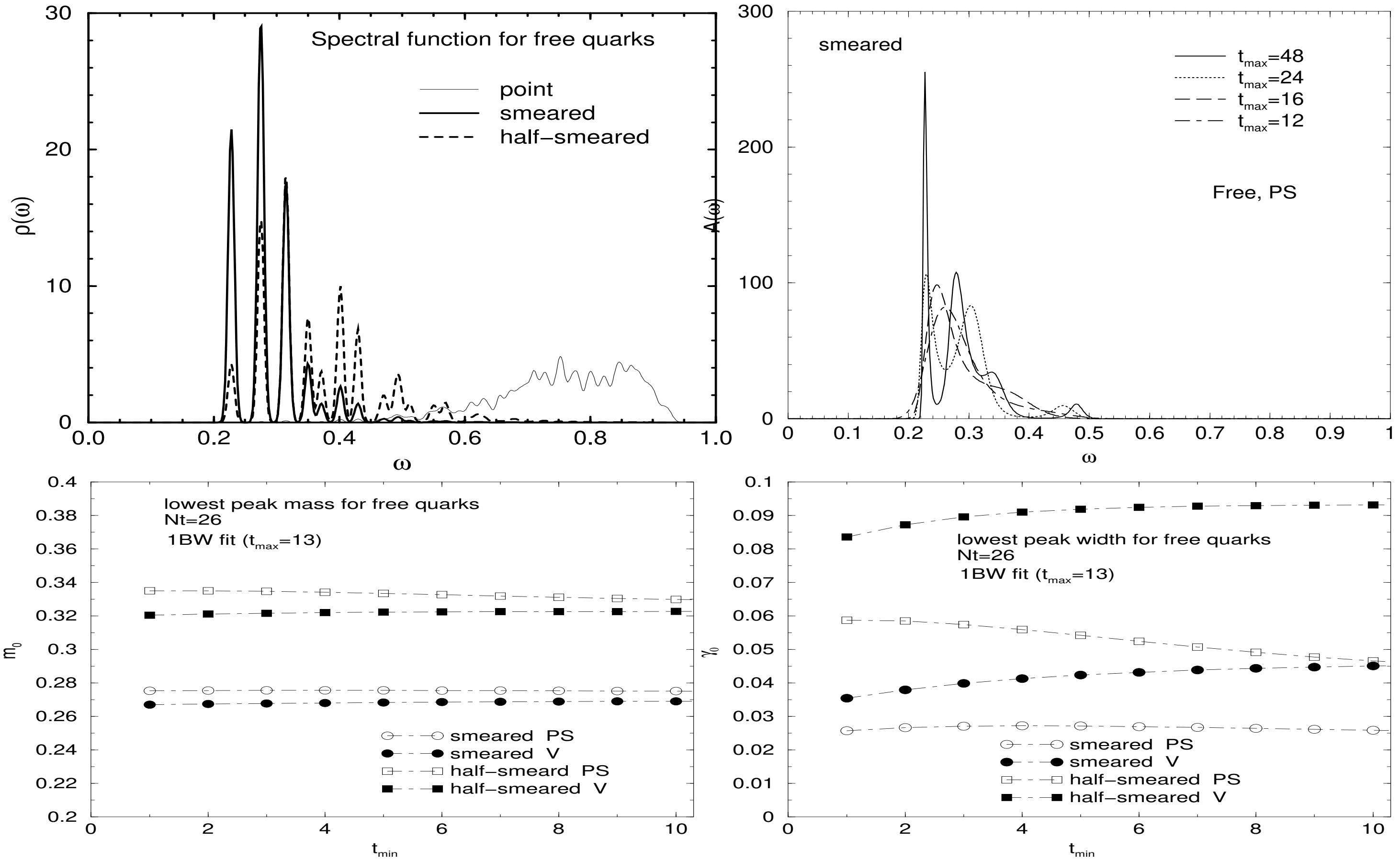

Figure 7: Upper plots: "Free" meson on $20^3 \times 160$ lattice, $a_\tau^{-1} = 8$ GeV. *Left plot*: Exact $\rho_0(\omega)$, given for various smearings. The low energy region is enhanced by smearing. *Right plot*: MEM recalculation of $\rho_0(\omega)$ using the first t_{max} points in $G_0(t)$. With decreasing t_{max} the structure is worse resolved and the peak position starts shifting since we only see the envelope. Lower plots: II. Fit for "Free" *ps* and V mesons on the $20^3 \times 26$ lattice ($T = 1.1\, T_c$). Insufficient smearing gives higher mass (*Left plot*) and width (*Right plot*) of first peak, since the low energy region is less pronounced.

The conclusion is that one should use smeared operators and $N_\tau > 2 \times 12$.

Spectral function at $T = 0$.

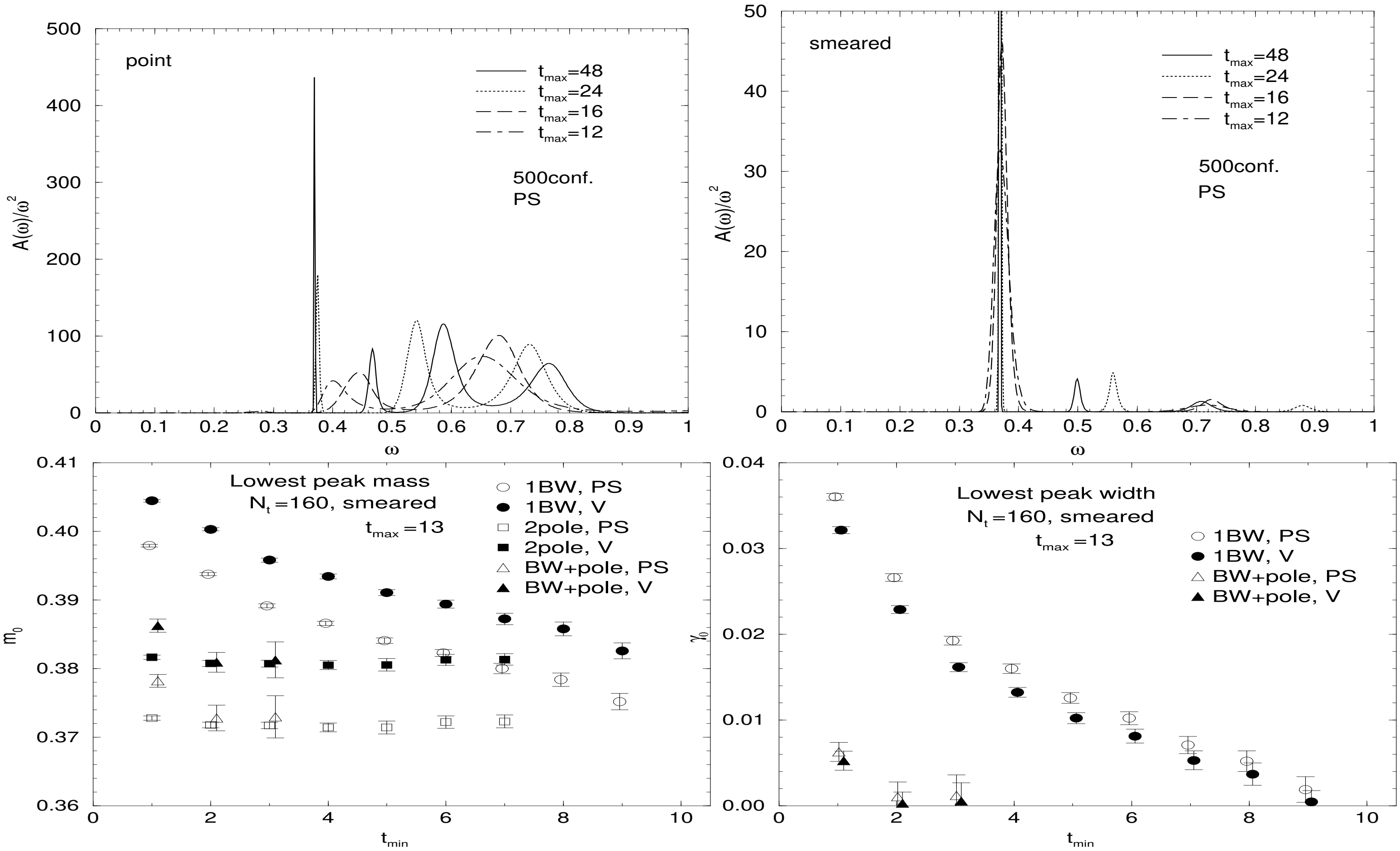

Figure 8: The *ps* meson at $T \simeq 0$, $20^3 \times 160$ lattice. Upper plots: I. MEM $\rho(\omega)$ for point (*Left plot*) and smeared operators (*Right plot*) using the first t_{max} points in $G(t)$. Lower plots: II. Fit with various *ansätze* to the *ps* and V propagators, using $t_{max} = 13$: peak position and width *vs* t_{min}.

I. MEM: With point operator reliable estimation of the first peak position (and width) is possible only for $t_{max} > 20$. The smeared operator gives stable estimation of the peak position for $t_{max} > 12$, while the width is overestimated for $t_{max} < 20$.

II. Fit: Already with $t_{max} = 13$ all *ansätze* give reliable position and width if t_{min} is large enough; 2 poles or Breit-Wigner and pole are optimal (less dependent on t_{min}.

The $T = 0$ analysis confirms that one must use smeared operators and $N_\tau > 2 \times 12$ in MEM to get at least the first peak position correct. MEM with t_{max} large enough agrees with the fit method.

Spectral function at $T = 1.1\,T_c$.

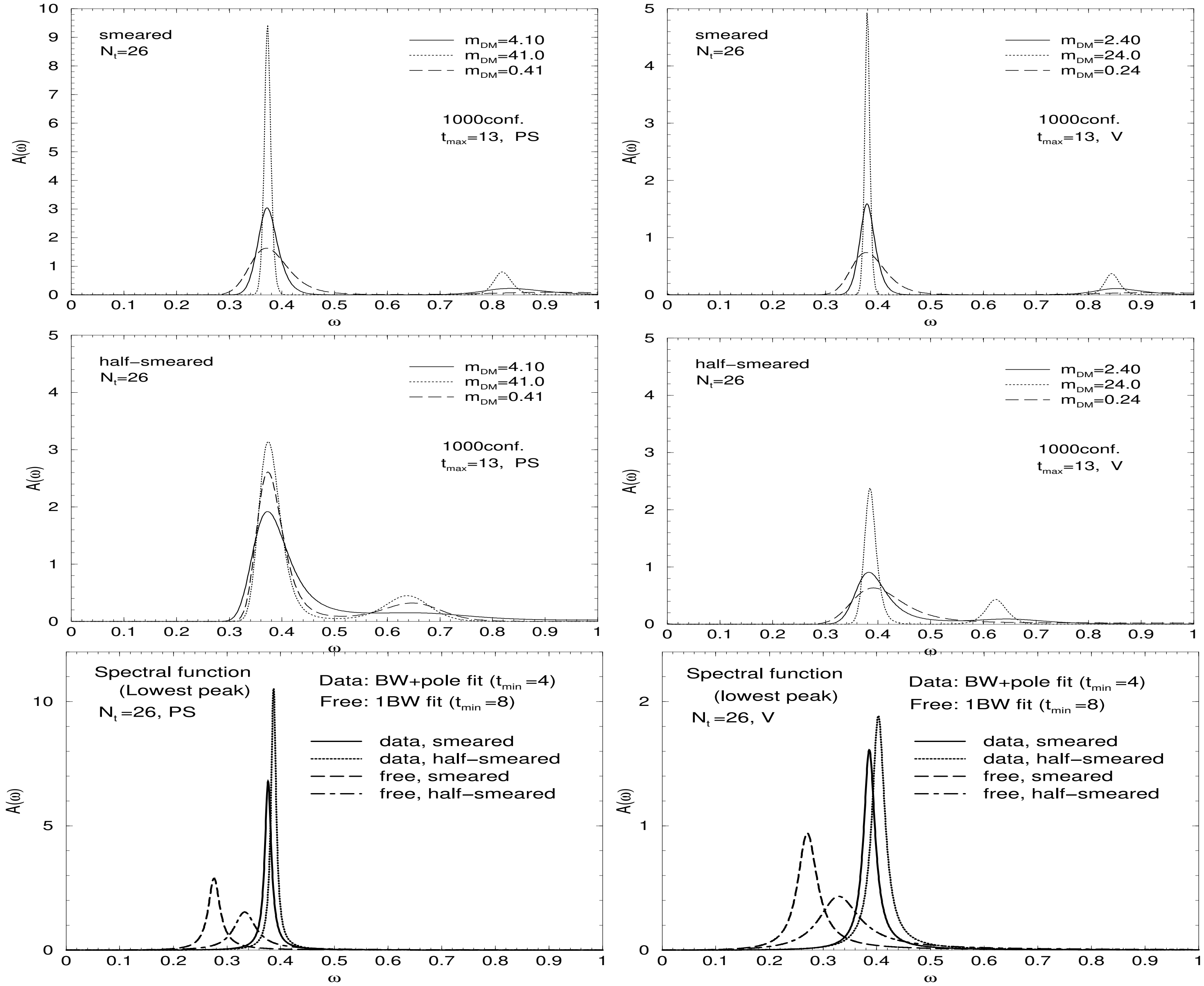

Figure 9: The *ps* (left plots) and V (right plots) at $T \simeq 1.1\,T_c$, $20^3 \times 26$ lattice for various smearings. *Upper plots*: I. MEM $\rho(\omega)$ for various m_{DM}. *Lowest plots*: II. Fit $\rho(\omega)$ with "BW + pole" and $\rho_0(\omega)$ with "BW" *ansatz*.

Summary of results for spectral function:

MEM with unsmeared operators and $t_{max} < 24$ gives wrong results;

MEM for smeared operators and $t_{max} > 12$ MEM gives reliable results for lowest peak position, the width depends on default model. 1 BW and BW + pole fit gives consistent results for both position and width:

$Ps:\ m = 3.06(3),\ \gamma = 0.12(3); \quad V:\ m = 3.13(2),\ \gamma = 0.21(2)$ (GeV)

STATIC QUARK POTENTIAL: Results from *Simulation III*

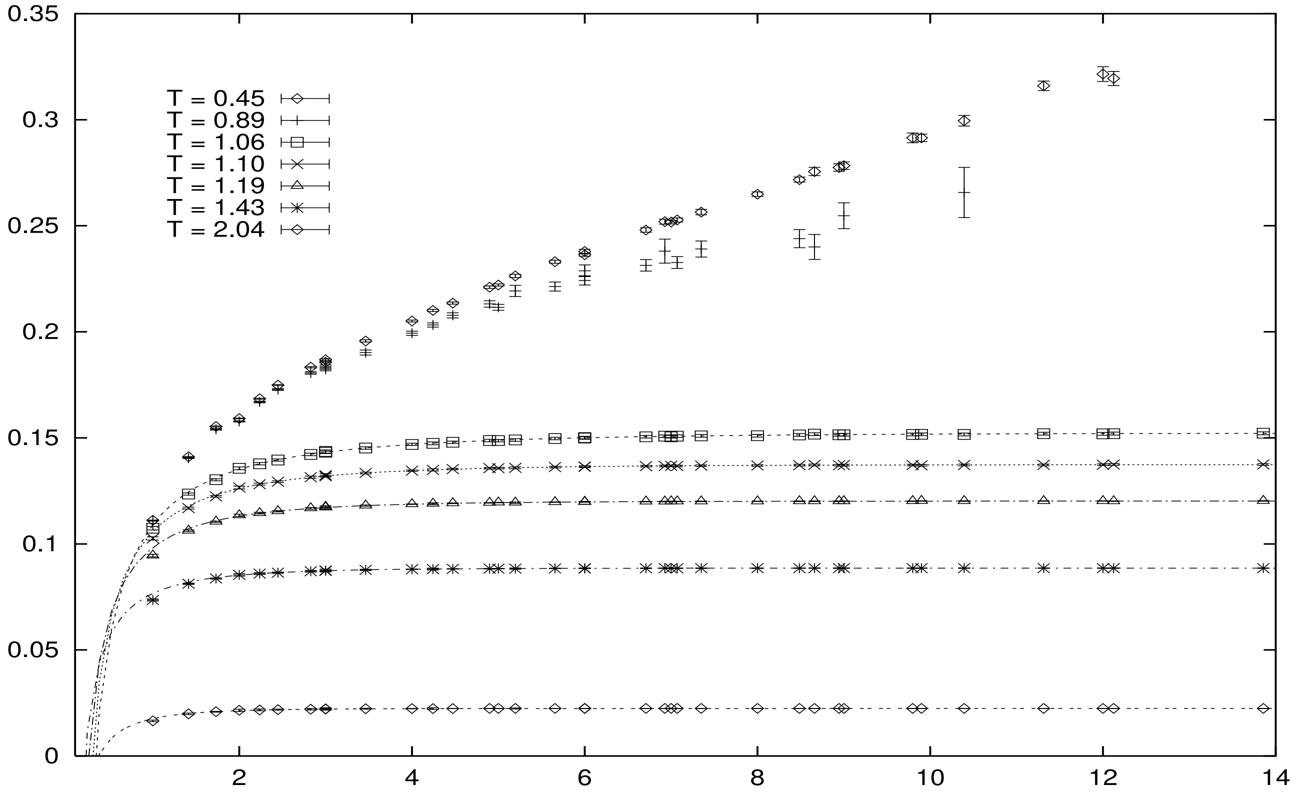

Figure 10: Static quark potential (vs r in units of $a_\sigma \simeq (2GeV)^{-1} \simeq 0.1$ fm) below and above T_c. The lines correspond to the fit:

$$V(r) = c - \frac{a}{r}\, e^{-\mu\, r}$$

<u>One observes</u>:

- rapid change in the large distance behaviour (above 0.2 fm) at T_c,
- slower change with T in the behaviour around ~ 0.1 fm.

$\mu(T)$ vs T from the fit is:

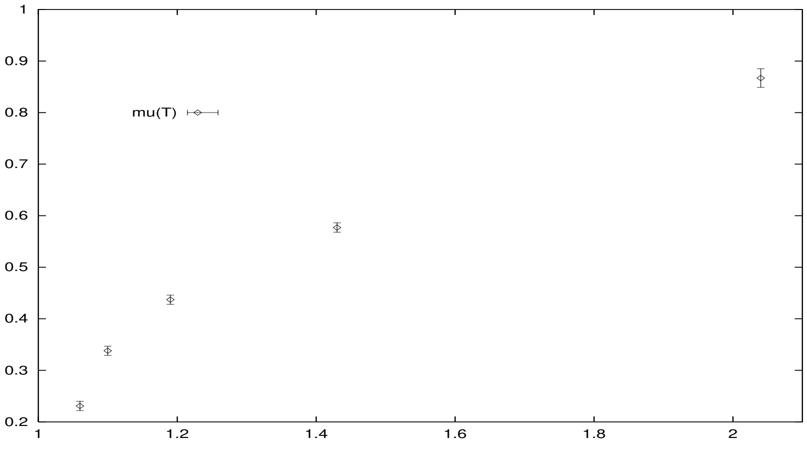

CONCLUSIONS AND DISCUSSION

Findings:

- Observation of well defined peaks in the spectral functions in the mesonic channels up to at least $1.1\,T_c$, and
- tendency of $q-\bar{q}$ to correlate spatially, as indicated by the stable wave functions up to at least $1.5\,T_c$,

  suggests persistence of mesonic (effective) excitations above T_c;
- The shape, the dependence on smearing, etc. suggests that above T_c the correlators are no longer dominated by one narrow state;
- Comparison with *perturbative QGP* shows both similarities and dissimilarities (the latter especially striking in the wave functions),

  suggests contribution from propagation of unbound quarks;
- "Light" mesons show chiral symmetry restoration at T_c and masses increasing linearly with T above T_c;
- Charm mesons show practically constant masses above T_c;
- The change in the static potential change at T_c is rapid concerning large distance, slow concerning short distance behaviour.

Tentative picture of QGP for $T \simeq 1. - 1.5\,T_c$:

Persistence of mesons above T_c as metastable states, together with increasing admixture of unbound but interacting quarks which acquire thermal masses via interactions in the plasma (manifest for light, less for heavy quarks).

Remarks:

Strong interactions of the quarks above T_c and widening of the structure in the spectral functions have also been found in a number of other studies in the last years (*Bielefeld group*, groups in Japan, etc). Wave functions at $T > T_c$ from temporal correlators have not yet been measured elsewhere.

Discussion:

- The shape of the Euclidean propagators (effective mass, etc) is an indicator for changes in the physics of the hadronic channels, but cannot differentiate between various effects (increased admixture of excited states, wide peaks, continuum contribution). The clear onset of these changes at T_c tend to discard the first explanation.

- The comparison of the propagators in the various channels support chiral symmetry restoration at T_c, however this is a quenched calculation and moreover the disconnected part of the S meson has not been taken into account.

- Smearing of the propagators seems to strongly help the analysis while local operators give results much too sensitive to the method (e.g., number of points). The former has been shown to enhance the low energy region in the spectral function and help therefore identify the low energy excitations, both for <u>Fit</u> and <u>MEM</u> procedures. Also, the study of the source dependence seems to give hints about the character of the states in the corresponding channels. A systematic understanding of the smearing effect is not yet available, however. But it is important that one uses a smearing which identifies the states by their internal structure, and checks for the self-consistency of the identification (stability of the wave functions).

- Both <u>Fit</u> and <u>MEM</u> procedures become uncertain if the number of time slices used is smaller than ~ 12 ($N_\tau < 24$). We did not pursue a systematic analysis on many lattices, nevertheless this limitation seems at least partly if not mainly related to the *physical length* $\simeq 1/T$ and thus indicate a difficulty of principle for analyses at large T (although also the increase of the number of points – e.g., by using anisotropic lattices – has positive significance).

- Cross checks between, and sensitivity checks inside various procedures (<u>MEM</u>, <u>Fit</u>) enhance the credibility of the results. Nevertheless with increasing T above T_c the quality of the latter deteriorates and even semiquantitative predictions become unreliable.

- The region between 1 and $2\,T_c$ appears as very interesting and structured. It seems that both more precise data and further development of the methods are required to approach this region. For instance, a combination of MEM and Fit method (using iteratively fit-*ansätze* as default model with selfconsistency criteria) might help obtain a reliable spectral function.

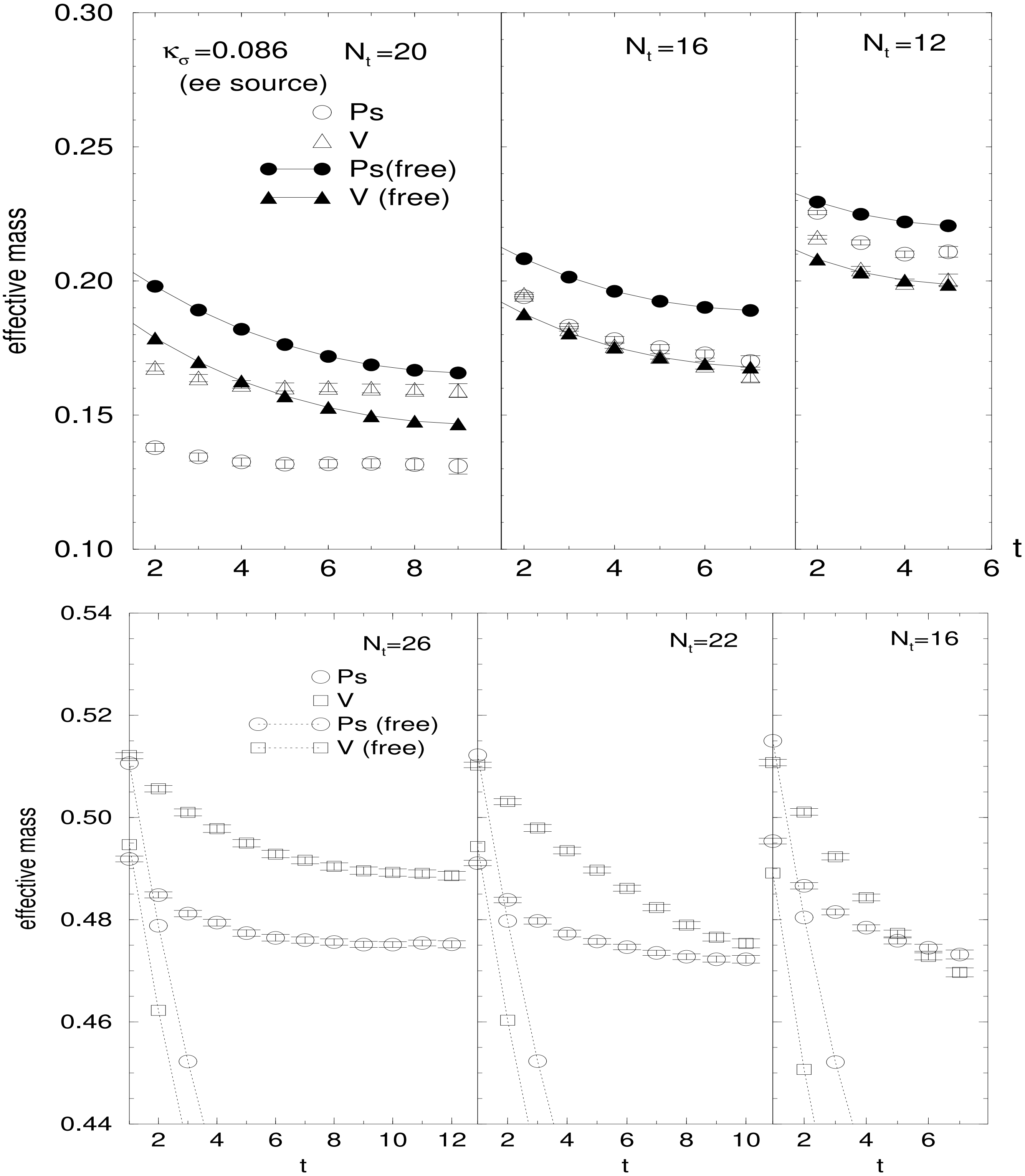

Figure 12: $\underline{T \simeq 0.93,\ 1.1 \text{ and } 1.5 \times T_c}$ (from left to right): Effective masses $M(t)$ for "light" quarks (*Simulation I*, upper plot) and "charm" (*Simulation II*, lower plot) for *ps* and vector mesons and *(ee)* source. Also shown are the "free quark mesons" using thermal quark masses $m_q^{therm} \propto T$ (fitted to reproduce the large T, vector meson data) in the upper plot, or $m_q = 0$ in the lower plot. Notice the hierarchy inversion between pseudoscalar and vector at high temperature: this also indicates with T increasingly wide structure in the spectral function.

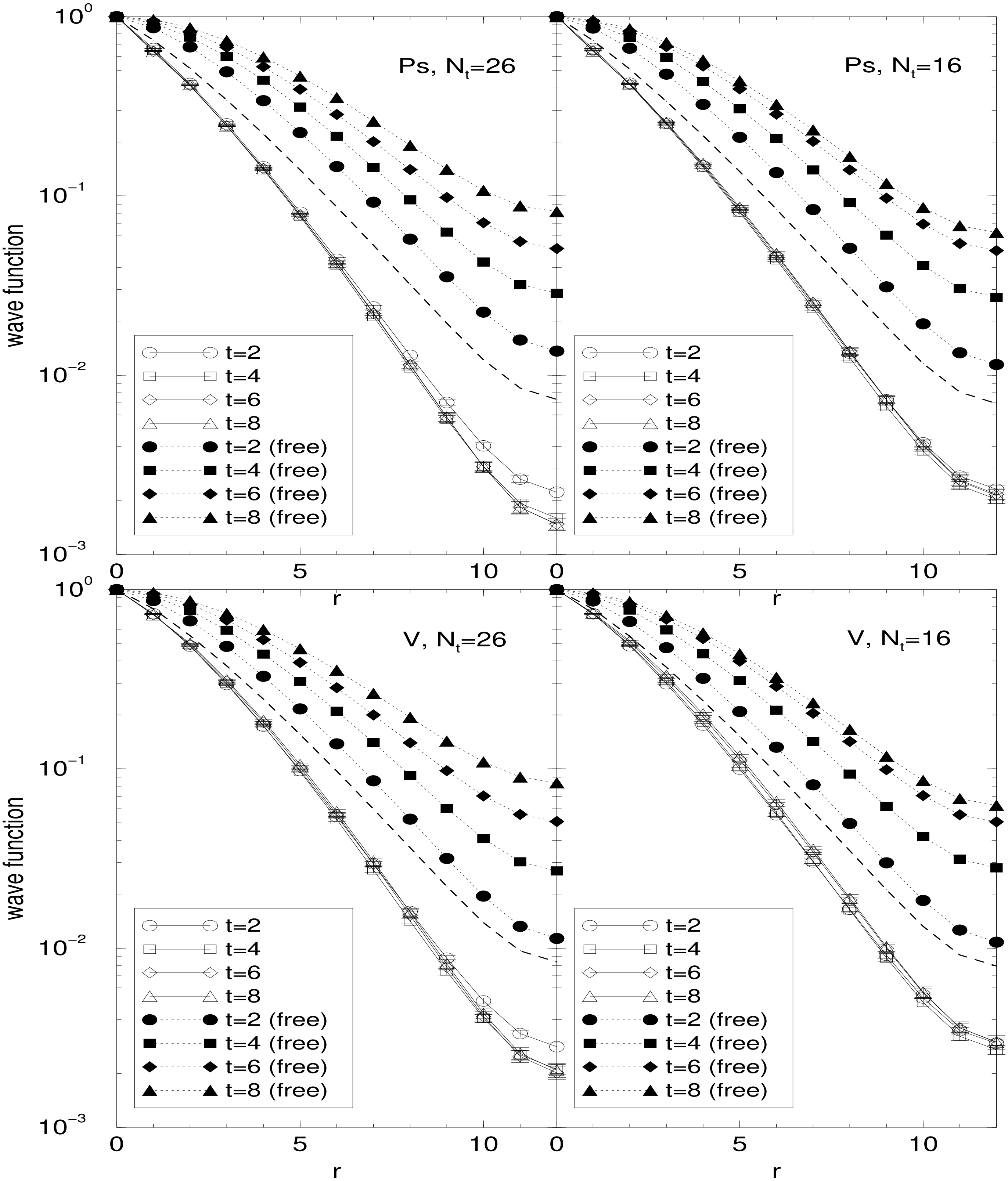

Figure 13: Wave function $\varphi(r,t)$ for charm (*Simulation II, (ee)* source) at $T \simeq 0.93$ and $1.5\,T_c$ (from left to right) at $t = 2$, 4, 6 and 8, for pseudoscalar (upper plot) and vector (lower plot), and free "wave function" $\varphi_0(r,t)$ (full symbols). Again we observe stabilization of the wave function, for both *ps* and V mesons, and both below *and above* T_c (while free quarks fly apart). The dashed line is the (ee) source ($t = 0$).

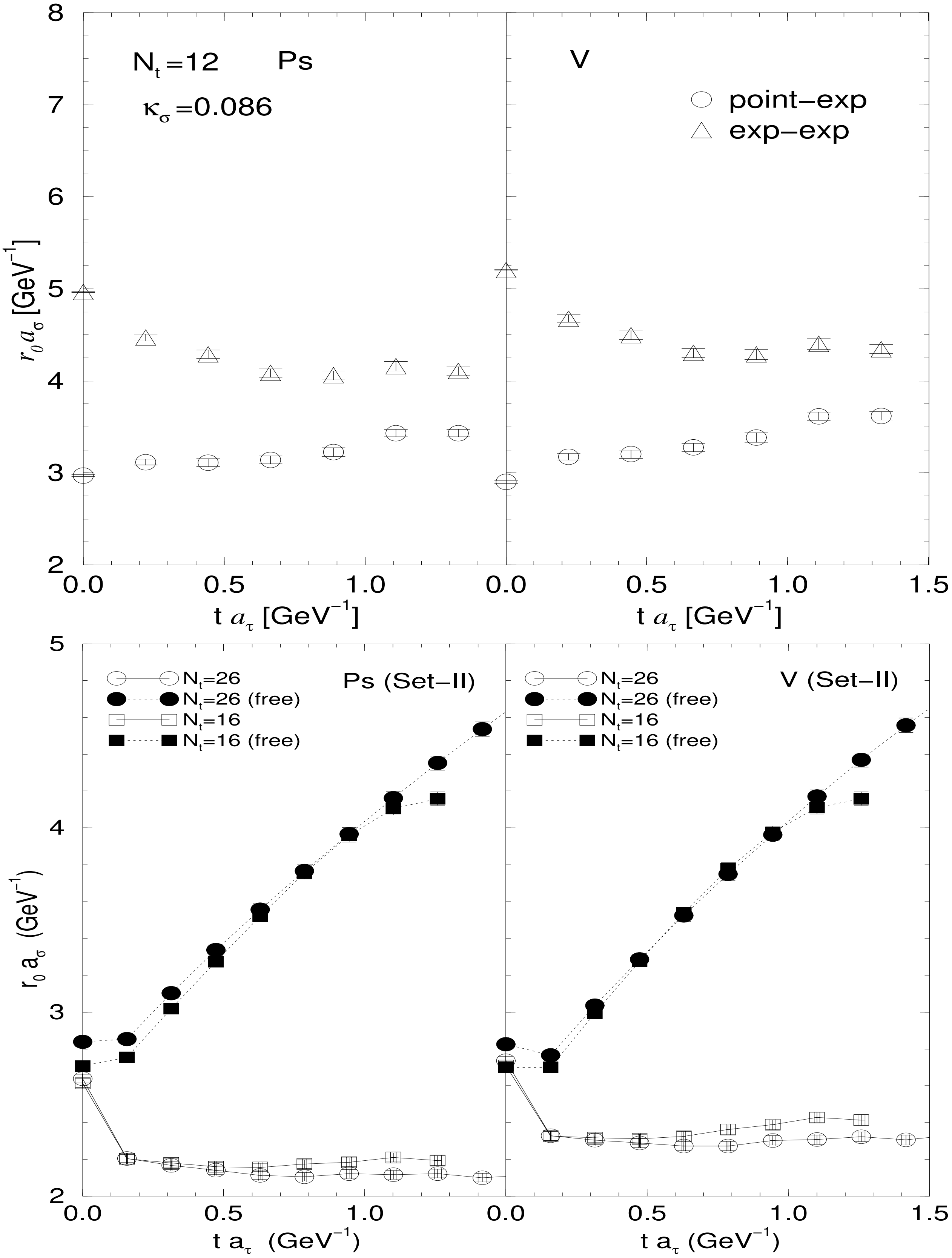

Figure 14: Evolution of the average distance r_0 between $q - \bar{q}$ with t for pseudoscalar (left) and vector (right). Upper plot: *Simulation I*, $T = 1.5\,T_c$, various sources. A narrow initial distribution widens, a wide one narrows, tending toward (but not yet reaching) a common limit. Lower plot: *Simulation II, (ee)* source. The $q - \bar{q}$ distance stabilizes both below and above T_c, while free quarks (full symbols) fly apart.